

# Fracture Detection from Pre-Stack P-wave Data

M. de Rooij<sup>1</sup>, N. Hemstra<sup>1</sup>, R. van Boom<sup>2</sup>

<sup>1</sup>dGB - de Groot - Brill Earth Sciences BV, Boulevard 1945 - 24, 7511 AE Enschede, The Netherlands,

<sup>2</sup>Wintershall AG, Postfach 104020, Kassel D-34112, Germany.

## Introduction

Fracture systems are notorious for causing reservoir performance uncertainties. Therefore, it is of vital importance to gain insight into a fracture system. In a fractured medium P and S-waves travel faster in the fracture strike direction than perpendicular to the fracture orientation (e.g. Rüger and Tsvankin, 1997). In general, S-waves are more sensitive to fractures than P-waves especially in case of open, fluid-filled fractures. Ideally, the study of anisotropy is conducted on S-wave data. However most surveys only record P-waves. Although less sensitive, anisotropy in P-wave data is a valuable instrument for detecting fracture density and orientation.

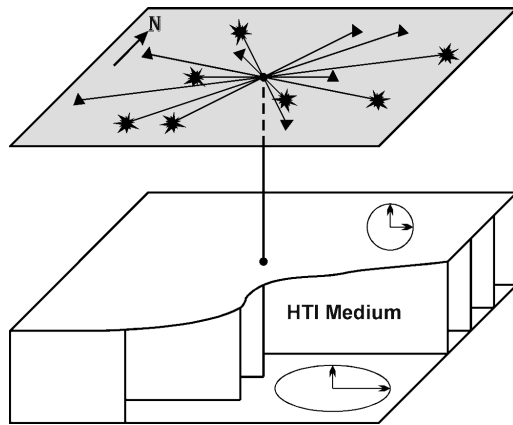


Figure 1.  
An HTI medium represents a fractured reservoir, the overburden is isotropic. The ellipses indicate the shear velocity in each medium. Source and receiver locations are sketched at the surface

## Methodology

The core of our approach is separation of the major factors that affect amplitude behavior in an anisotropic medium: the common AVO effect and the reflectivity vs. azimuth effect. The dominant offset-related variations in amplitude are separated and removed yielding a variation, which contains the essential information on anisotropy. We assume a model with isotropy above an HTI medium (Figure 1).

First the amplitudes of a single event in a pre-stack gather are extracted. Azimuth information of each trace needs to be preserved. We calculate the AVO gradient and intercept of the event. We then postulate that the relative differences between the AVO gradient line and the actual data points represent the azimuthal variation of P-wave reflectivity. These relative differences are the equivalent of relative difference between the circle (isotropy) and the ellipse (anisotropy) from Figure 2. By fitting the equation of an ellipse to these data, the ratio of the long and the short axis of the ellipse and the azimuth of both axes can be established. These two parameters describe the anisotropy of the reflectivity.

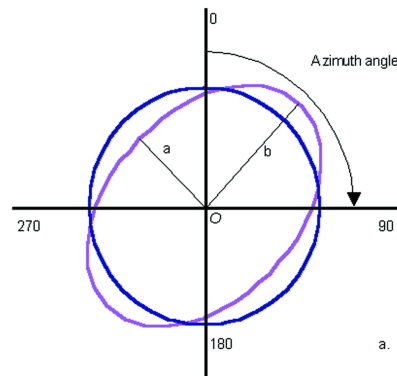


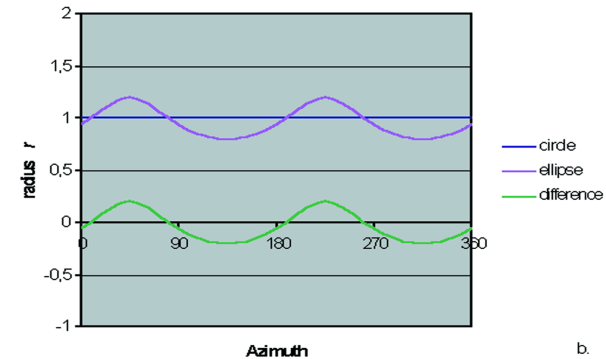
Figure 2.  
Ellipse representing the variation of properties with azimuth, the circle represents isotropy. (a) polar plot, (b) the same circle and ellipse, but in orthogonal plot and including the difference.

## Seismic data

The method is tested on realistic synthetic gathers, created with real P-wave sonic and shear wave logs from a well in a fractured reservoir. Sonic and shear log data from a vertical well in a fractured reservoir is used as a starting point.

Different scenarios are simulated. Model 1 represents an East-West fracture system with maximum shear log reduction of 10%. Model 2 exhibits a maximum shear log reduction of 5%. To analyze a potential bias of uneven offset and azimuth distributions per gather, the far offsets for both models are generated for 0deg or 90deg azimuth only.

Using a Zoeppritz-based pre-stack modeling algorithm, synthetic NMO corrected gathers are created covering all azimuths. Offset varies between 0 and 3000 m. The offset and azimuth distributions in the gathers are similar to real field gathers.



## Results

At the objective level, the amplitudes are extracted from the gathers (Figure 3). Offset and azimuth information is preserved. First, the AVO gradient and intercept are calculated (Figure 4). Next, the relative differences between the data and the AVO gradient line are determined and plotted against azimuth. The ellipse equation is fitted to this data by minimizing the R2 error (Figure 5). This fit yields the two parameters describing the anisotropy in reflectivity: the ratio of the length of the axes (a/b, see Figure 2) and the azimuth of the long axis. All results are summarized in Table 1.

Model	Gather orientation	Azimuth long axis		a/b	
		Input	Calculated	Input	Calculated
Base case	East-West	-	105	1	0.97
Model 1	East-West	0	4	0.60	0.74
Model 1	North-South	0	1	0.60	0.65
Model 2	East-West	0	8	0.80	0.91
Model 2	North-South	0	3	0.80	0.82

Table 1. Resulting anisotropy parameters, input and expectation based on Zoeppritz and a gather with full offset and azimuth coverage.

## Conclusions

- The method provides valuable quantitative information.
- The base case without anisotropy yields an a/b near 1.
- The long axis of the ellipse can be reconstructed regardless orientation of the gather.
- The a/b ratio is well resolved for the different models.
- In terms of fracture detection, a relation between a/b values and fracture density is very likely, and should not be difficult to find, even if such a relation is non-linear.

## Discussion

To improve the S/N ratio it is possible to filter the data and/or increase the number of data points. A common procedure in AVO analysis is the creation of super-gathers prior to computing attributes. This will lower the azimuthal resolution of the analysis though. The proposed method for quantifying anisotropy is very

promising. However, it needs testing on a real, preferably pre-stack migrated, pre-stack volume.

## Acknowledgements

We kindly thank the partners of the UTE San Roque (TotalFinaElf, Repsol YPF, Pan American Energy and Wintershall Energia S.A.) for permission to publish these results.

## References

- Mavko, G., T. Mukerji, J. Dvorkin, The Rock Physics Handbook, 1998, Cambridge University Press, Cambridge, U.K.  
 Rüger, A. and Tsvankin, I., 1997. Using AVO for fracture detection: Analytic basis and practical solutions. The Leading Edge, Oct. 1997.  
 Sheriff, R.E., and Geldart, L.P., Exploration Seismology, 2nd Edition, 1995, Cambridge University Press, Cambridge, U.K.

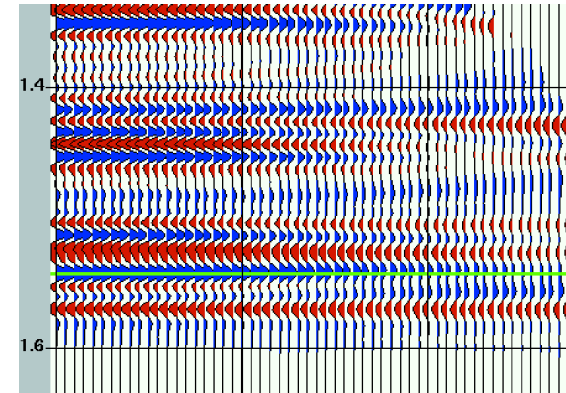


Figure 3. Amplitudes at the level of interest are extracted from the gather.

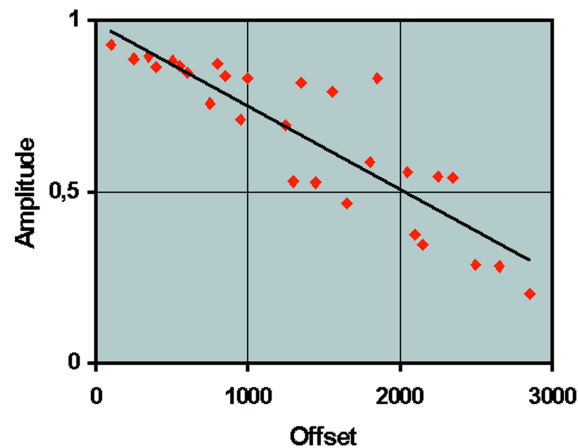


Figure 4. AVO plot of model 1, gather in East-West direction.

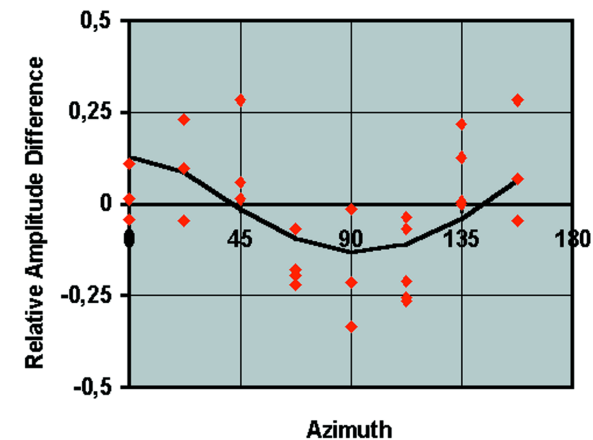


Figure 5. Fit of the ellipse equation to the relative differences from figure 4.